ORIGINAL RESEARCH

Efficacy and Sensitivity of Axial Scans and Different Reconstruction Methods in the Study of the Ulcerated Carotid Plaque Using Multidetector-Row CT Angiography: Comparison with Surgical Results

L. Saba
G. Caddeo
R. Sanfilippo
R. Montisci
G. Mallarini

BACKGROUND AND PURPOSE: Carotid plaque ulceration is an important risk factor for stroke, and its diagnosis may be very important to plan a correct therapeutic approach. We hypothesized that axial scans and various reconstruction methods could have different specificity and sensitivity in the study of plaque ulceration. The object of this study was to evaluate their role and diagnostic efficacy in patients with carotid plaque complicated by ulceration through the comparison with surgical results.

MATERIALS AND METHODS: From January 2004 to November 2005, 109 patients who underwent a carotid endarterectomy were analyzed using CT angiography for a total of 218 carotid arteries. We assessed every carotid for the presence of ulcerations. For each patient axial image, maximum intensity projection (MIP), multiplanar reconstruction (MPR), shaded surface display (SSD), and volume rendering (VR) reconstructions were obtained.

RESULTS: Multidetector row CT angiography (MDCT) found 32 ulcerations; surgical confirmation underlined an overall 93.9% sensitivity (95% confidence interval [CI] 0.858–1.021), and a 98.7% specificity (95% CI, 0.961–1.012). Axial scans and volume rendering images demonstrated the highest sensitivity (90.9% and 87.9%, respectively); SSD, on the contrary, showed the lowest sensitivity: 39.4% (95% CI sensitivity, 0.227–0.561).

CONCLUSION: Axial scans plus VR reconstruction techniques offer superior depiction of carotid plaque ulceration compared with MIP, MPR, and SSD.

It is well known that stroke is one of the leading causes of severe disability in the Western world,[1] and it represents the second highest cause of death worldwide.[2,3] Extracranial carotid artery stenosis is accepted as a significant risk factor for cerebrovascular events, but patients with atherosclerotic disease may be at higher risk depending on plaque morphology and the presence of its complications, such as ulcerations.[4,5] Consequences of plaque ulceration have been clearly underlined in the North American Symptomatic Carotid Endarterectomy Trial (NASCET)[6]: this situation represents an important risk factor for neurologic symptoms,[7] so that a high grade stenosis combined with plaque ulceration produces an increased risk of stroke.

In the past, conventional angiography has been considered the standard method for evaluating stenosis of the carotid artery, but if we focus on the study of ulcerated plaque, this technique has been demonstrated not to be sufficiently reliable.[8-11] Sometimes, in fact, angiography is not able to detect small ulcers. Moreover, conventional angiography is frequently associated with a risk of thromboembolic events because of the use of an arterial catheter.[12] So, if we analyze the risks and costs of this procedure, noninvasive techniques, such as CT angiography (CTA), have recently been becoming more and more important. The use of multidetector row CT angiography (MDCT) along with workstations and sophisticated software is getting greater consensus as a valid and sensitive 2nd-level method to study the carotid artery and its complications, because it always introduces a greater spatial resolution, avoiding the risks of digital subtraction angiography (DSA).[13]

To study carotid arteries and other vessels using MDCT, it is possible to use different techniques of postprocessing in addition to axial scan: maximum intensity projection (MIP), multiplanar reconstruction (MPR), shaded surface display (SSD), and volume rendering (VR)[14,15] are the most frequently used nowadays. First introduced in the late 1980s, postprocessing methods currently show an impressive visual capacity of representing anatomic structures, but they are not always adequate in detecting and visualizing all pathologic conditions. Therefore, they have to be used critically to obtain the best diagnostic efficacy. Besides, there are many types of image reconstructions available, and we believe that the simultaneous use of all of these tools is time-consuming and incorrect. We hypothesized that axial scans and various reconstruction methods had different specificity, sensitivity, and depiction capacity in the study of plaque ulceration. The purpose of this study was to evaluate their role and diagnostic efficacy in detecting carotid plaque complicated by ulceration compared with surgical results.

Received June 7, 2006; accepted after revision August 3.

From the Departments of Imaging Science (L.S., G.M.) and Vascular Surgery (R.S., R.M.), Policlinico Universitario, Cagliari, Italy; and Institute of Radiology (G.C., G.M.), University of Cagliari, Cagliari, Italy.

Address correspondence to Luca Saba, Department of Imaging Science, Policlinico Universitario, s.s. 554 Monserrato (Cagliari) 09045 Italy; e-mail: lucasaba@tiscali.it

Materials and Methods

Patients

From January 2004 to November 2005, 109 surgical patients (71 men, 38 women; mean age, 68 years; range, 49–85 years) were studied using CTA, and these patients subsequently underwent carotid end-

arterectomy (CEA). Major criteria used to decide when to perform CEA were 1) patients with stenosis of more than 70%; 2) symptomatic patients with stenosis of more than 50% with presence, on songraphic echo-color-Doppler and CTA, of images of intraplaque hemorrhage, fissuration, or irregular surface; and 3) symptomatic patients with ulceration. Seventy patients showed symptoms related to carotid artery lesions, including transient or persistent monocular visual loss, hemispheric transient ischemic attacks (TIAs), and ischemic stroke; 39 patients were asymptomatic. First, all our examinations were interpreted as part of clinical work-up. In a second phase, we randomized all the 109 examinations and CTA images were reinterpreted by the radiologists.

CTA Technique

The angiographic CT examination was performed with a multidetector row spiral CT scanner (Somatom Mx8000; Siemens, Erlangen, Germany). To determine the level of carotid bifurcation and the possible presence of calcifications, we performed a scan without contrast material in 5-mm sections from C2 through C6.[16,17] Then we started angiographic acquisition. Arterial enhancement was provided by the intravenous administration of 130 mL of nonionic iodinated contrast material (iopromide [Ultravist 370]; Schering, Berlin, Germany) at an injection speed of 4 mL/s. We used a delay time between 15 and 18 seconds. Spiral images were acquired with a table speed of 3 mm/s and a 3-mm collimation. CT technical parameters included: matrix, 512 × 512, FOV, 12–19 cm; section thickness, 1.6 mm. The scan started at the C7 and proceeded as far cephalad as possible, including carotid siphon. Total examination time, including patient preparation, was between 10 and 20 minutes. Axial source images were reconstructed in 1.6-mm increments using a 14-cm FOV. Axial images were analyzed with various zoom levels from 20%–100% compared with the acquisition. The window level was preset at 200 HU with a width of 700. Reconstructed images were processed using our workstations (Figs 1, 2, and 3).

Postprocessing Procedures

Reconstructed images were processed using MPR, SSD, MIP, and VR algorithms. In the MPR,[18,19] we generated multiple projections for each dataset, and radiologists could manipulate both the window, the center, and the view angle. In both MIP[20] and SSD, regions of interests (ROIs) were selected by manual drawing to exclude bone structures, which might be superimposed over the carotids. Moreover, we did not use a preset window level or window width in the MIP images, giving radiologists the opportunity to choose according to their preferences.

In VR image generation, we[21] initially selected 2 trapezoids to display the contrast material-enhanced arterial lumen (lumen trapezoid) and the mural calcifications (calcification trapezoid). The window width and level were chosen in an empirical manner, as described by Leclerc et al.[16] We usually selected voxels ranged in a window from 280 to 400 HU for the lumen trapezoid and from 800 to 1200 HU for the calcification trapezoid. If we identified an image that was indicative of ulceration, we activated a third trapezoid that pointed out endoluminar contrast material with a window ranging between 400 and 800 HU (contrast trapezoid).

Image Interpretation and Definition of Ulceration

Grade of stenosis and presence or absence of ulcerated plaque, using the different postprocessed images, were classified by 2 observers in consensus. We used the presence of an "in plus" image larger than 1 mm as an imaging criterion to define an ulceration. In axial images, we considered the presence of a visible plaque into which ulcer projects a second criterion to identify an ulcer. At the beginning, we randomized all patient data; the 2 observers could see only axial images and their results were registered. After 14 days, the whole MIP dataset was analyzed, and at 2-week intervals, the MPR, SSD, and VR datasets were studied. Corresponding evaluations were registered. At the end, access to all reconstructions and images was allowed, and results were acquired. We applied this procedure to avoid the possibility that the memory of previous evaluations would influence the later ones. Our purpose was to obtain a reliable assessment of positive predictive value (PPV), negative predictive value (NPV), sensitivity, and specificity according to the different reconstruction techniques.

Stenosis Degree, Plaque Types, and Morphology Evaluation

Each carotid artery was graded according to the NASCET criteria.[6] To quantify degree of stenosis,[22] measurements were made on a strictly perpendicular plane to the carotid axis to define the exact orientation in the space. The value was calculated by comparing the diameter of the stenosed segment with the more normal distal segment when no stenosis was present and by using the MIP projection when the degree of stenosis was larger.

Moreover, we studied different plaque types by using axial scans, and we divided plaques into 3 different groups according to Schroeder et al[23]: *fatty plaques* had attenuation values less than 50 HU; *mixed plaques* had attenuation values between 50 and 119 HU; and *calcified plaques* had attenuation values greater than 120 HU. The attenuation of Hounsfield units was measured with the use of a circular or elliptical ROI cursor in the predominant area of plaque at each level.[11]

We divided plaques into 3 morphologic types: perpendicular, button of shirt, and hook. In the *hook* morphology, the ulcer neck is proximal or distal, and the main part of the ulcer points in the direction opposite that of the neck (ie, distally or proximally, respectively) (Fig 1). In the *button of shirt* morphology (Fig 2), the ulcer has a narrow neck and this aspect in axial images is displayed as a dissectionlike image. In the *perpendicular* morphology, the ulcer comes out perpendicular to the lumen with a neck wider than the fundus (Fig 3).

Surgical Specimens

For all patients, we had surgical specimens provided by vascular surgeons. Surgical plaques were obtained "en bloc." To precisely confirm spatial localization of the ulcer to enable comparison with the CTA images, all surgical specimens were marked. To orient the specimen, we marked the medial or lateral position, depending on the surgical approach. Then the position of internal carotid artery (ICA), external carotid artery (ECA), and common carotid artery (CCA) in the surgical specimen was analyzed, annotated, and compared with VR to acquire more information about spatial position and relationship. After the analysis of the specimens, surgeons indicated the presence or absence of ulceration. The surgical criterion for defining ulceration was the presence of discontinuation and macroscopic loss of integrity of the intimal layer approximately 1 mm or more in diameter and depth. If an ulcer was detected, surgeons indicated its position. The examination of the atheromatous plaques was made grossly, and the presence or absence of ulcerated plaque was classified by 2 experienced vascular surgeons in consensus.

Fig 1. A 71-year-old man with persistent monocular visual loss. VR (*A, B*), MIP (*C*), and axial scans (*D*) show a severe and irregular ulcerated plaque of the internal carotid artery (ICA). In the left ICA, proximal to the point of maximum stenosis (60% NASCET), is clearly depicted an ulceration of 2 mm (*red arrows*). In the VR images, *A* is set *without* contrast media histogram and *B* is set *with* contrast media histogram. In *C*, there is visible hook morphology (ICA, *blue arrow*).

Statistical Analysis

We assessed on axial scans the MIP, MPR, SSD, and VR for the following parameters: sensitivity, specificity, PPV, and NPV, and their confidence intervals (CIs), in the evaluation of ulceration of carotid plaque, by comparing imaging observations with surgical specimen results. To produce these data, we used spreadsheet software (Excel 2003, Microsoft, Redmond, Wash).

Results

Ulcer Detection Using CTA and Surgical Specimens

In the 109 patients who underwent carotid endarterectomy, we identified 32 plaque ulcerations at CTA as part of the patient's clinical work-up. The total number of ulcers identified by surgeons, when removed plaques were analyzed, was 33. Of the 32 ulcers previously detected using CTA, 31 were confirmed by surgery. Surgery also detected 2 ulcers not previously identified by CTA. One ulcer indicated by the radiologist was not detected by surgeons when endarterectomy was performed. The overall CTA sensitivity in detecting ulcerated plaque was 93.9% (95% CI sensitivity = 0.858–1.021) and the specificity was 98.7% (95% CI specificity = 0.961–1.012)

Axial Scans and Reconstruction Methods Performances

After we collected the surgical specimen results, all 109 CTA cases were randomized and reinterpreted by evaluating only the axial images. Thirty ulcers were detected (of 33 in total), and we indicated a further 4 ulcers that were not confirmed by surgery. Sensitivity obtained was 90.9% and specificity was 94.7%.

Axial scan reached optimal results in detecting ulcerated plaque with the exclusion of ulcers located in calcified type plaques (2/4). By using MIP postprocessing methods, we detected 26 ulcers (of 33 in total), and we indicated 6 ulcers that were not confirmed by surgery. Sensitivity and specificity were 78.8% and 92.1%, respectively. In the MPR image evaluation phase, we detected 25 ulcers (of 33 in total), and we found 7 false-positives that were not confirmed by surgery. Sensitivity was 75.8% and specificity was 90.8%. MIP and MPR reconstruction modalities showed similar capacity to depict the ulceration.

The SSD method showed a poor capacity to depict ulceration in the carotid plaque, as evidenced by the large number

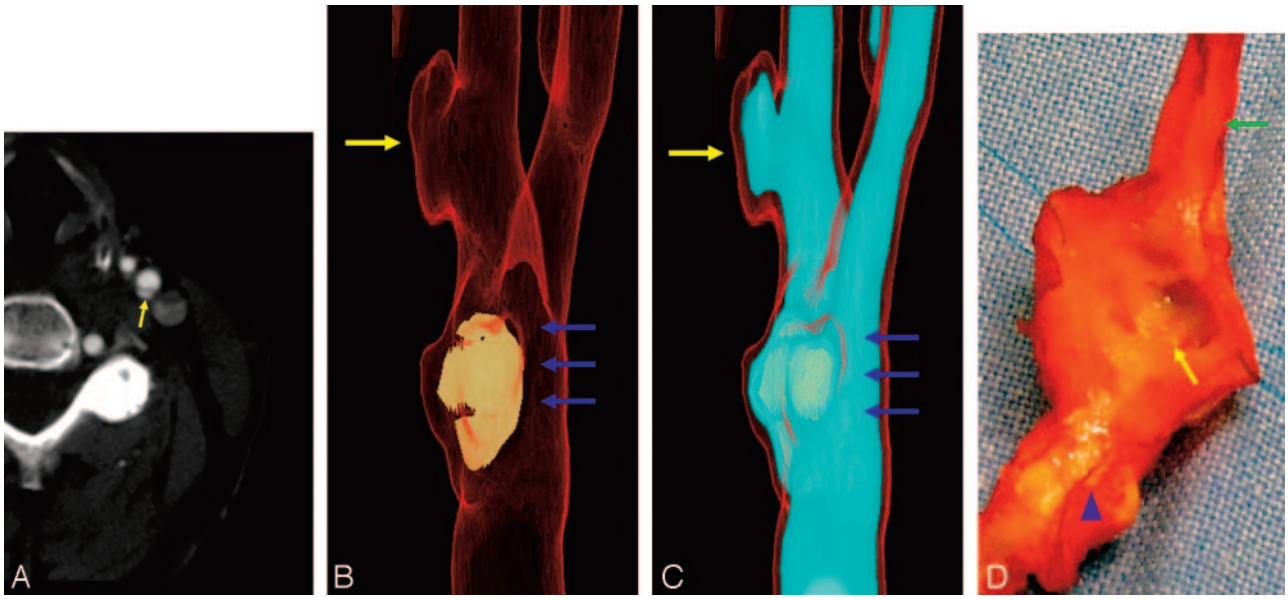

Fig 2 A 65-year-old woman with TIA. Ulcerated plaque of the left internal carotid artery (ICA); the typical *button-of-shirt* morphology is visible. Axial scan (*A*) illustrates ulcerations in a mixed plaque and displays a dissectionlike aspect. VR (*B, C*) clearly depicts the ulceration. Gross anatomic inspection confirms the presence of the ulcer (*D*). In this patient, the plaque is heavily calcified proximally and is not calcified at the location of the ulcer. This ulcer is distal to the point of maximum stenosis located in the bifurcation (80% NASCET), and could also have been a pseudoaneurysm from carotid dissection, but the surgical specimen confirmed the presence of ulceration. Note the big plaque calcification located in the bulbus/bifurcation (*yellow arrows*, ulceration; *blue arrows*, maximum stenosis point; *green arrow*, ICA; *blue arrowhead,* calcified plaque). The external carotid artery ostium is not visible because the cut plane passed through it.

of false-negatives; in fact, when we analyzed SSD reconstructions, we detected only 13 ulcers (of 33 in total) and we indicated as well 9 ulcers that were not confirmed by surgery. Sensitivity was the lowest among all the postprocessing techniques: 39.4%.

VR reconstruction methods showed the best results in detecting ulceration compared with the other postprocessing algorithms. Using VR we detected 29 ulcers (of 33 in total), whereas only 2 MDCT-detected ulcers were not confirmed by surgery. Sensitivity was 87.9% and specificity was 97.4%. VR technique reconstruction showed the best capacity to detect ulceration compared with the other postprocessing tools. Table 1 and Figs 4, 5, and 6 summarize these results.

Stenosis Degree, Plaque Types, and Ulceration Morphology Evaluation

Plaque type category (fatty, mixed, and calcified) and degree stenosis are illustrated in Table 2 and Table 3. We detected 10 ulcers with perpendicular morphology, 12 with button of shirt morphology, and the remainder showed a dissected morphology.

Discussion

Detection of plaque ulceration may lead to a modification of therapeutic approach from medical treatment only to surgery, when clinical signs and symptoms are consistent, so the application of a proper imaging technique becomes essential. DSA was not sensitive in detecting plaque ulcerations[8-11] and, moreover, it may cause severe complications,[17,24] though in the past few years, DSA has been widely used to study carotid arteries and their complications, as ulceration.[25,26] For these reasons, in our study, surgical comparison and not DSA was chosen as standard reference. We could find only a few works in which plaque ulceration with CTA was accurately studied; normally, in fact, ulcerations are reported among various data in works about carotid artery.[8,11,24,27-29] To our knowledge, the study of carotid ulceration with CTA is still a topic not sufficiently considered in the literature. Our specific approach may therefore explain our results that show a higher sensitivity if compared with the data of Oliver et al,[24] Walker et al,[11] Link et al,[29] and Schwartz et al.[27]

In this study, we assessed the capacity of 4 different types of reconstruction algorithms and axial scans to detect carotid ulceration. We wanted to define the most efficient algorithms to use, in a better and more selective way, the multiple potentialities offered by the newest graphic workstations.

Axial scans demonstrated 90.9% sensitivity in detecting the presence of plaque's ulcerations. When we found larger ulcerations (more than 3 mm), the sensitivity was even higher (7/7). Only in small ulcerations localized in calcified plaque did we find some problems (2/4 identified). We believe that, for a correct evaluation of ulceration presence in axial images, it is important to use a center level and a window that allows the discernment of the parietal calcified component—when present—from contrast material. A comparison with basal scans[27] may sometimes be useful; usually, however, basal acquisition is generally obtained with parameters different from those used with contrast-enhanced scans, so it is not always possible to make a comparison.

MIP is a simple 3D visualization tool that can be used to display CTA data. MIP images are not threshold-dependent and they preserve all CT data. For a given viewing direction, parallel rays are cast through a volume of interest (VOI), and the maximum CT number encountered along each ray is displayed.[20] MIP reconstructions evidenced a 78% sensitivity. In 22% (7/33) of cases, MIP was not able to detect the presence of plaque ulceration. In 3 cases of calcified plaque, MIP did not detect the ulcer (identified 1/4). In the remaining 4 false-neg-

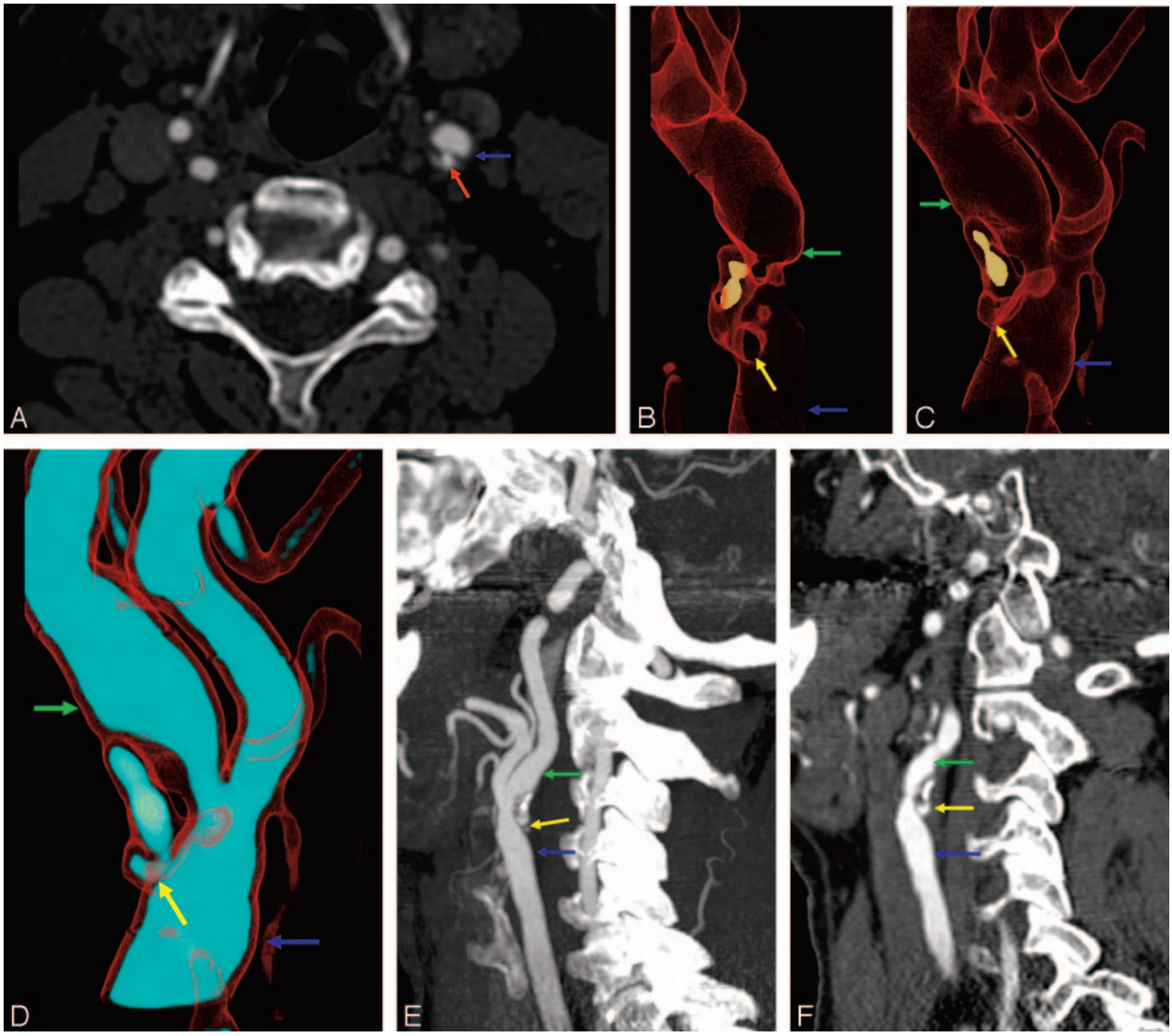

Fig 3. A 78-year-old man with TIA. Ulcerated plaque of the left CCA. Axial scan (*A*) shows ulcerations in a calcified plaque; the atheromatous plaque involved the common carotid artery, the carotid bifurcation, and internal carotid artery origin. This ulcer is proximal to the point of maximum stenosis (90% NASCET). The ulceration was easily detected using VR technique with 1 histogram (*B*) and 2 histograms (*C, D*). Ulceration was less clearly visible using MIP and MPR reconstruction (*E, F*). Note: *B* is an internal visual, where the lumen is cut to clarify the ulcers. (*red arrow in axial image and yellow arrows in VR, MIP, and MPR images*, ulceration; *green arrows*, ICA; *blue arrows*, CCA)

Table 1: Performances of axial scan and postprocessing techniques

Method of Evaluation	% Sensitivity (CI)	% Specificity (CI)	% PPV (CI)	% NPV (CI)
Axial scan	90.9 (81.1–100.7)	94.7 (89.7–99.8)	88.2 (77.4–99.1)	96.0 (91.6–100.4)
MIP	78.8 (64.8–92.7)	92.1 (86.0–98.2)	81.3 (67.7–94.8)	90.9 (84.5–97.3)
MPR	75.8 (61.1–90.4)	90.8 (84.3–97.3)	78.1 (63.8–92.4)	89.6 (82.8–96.4)
SSD	39.4 (22.7–56.1)	88.2 (80.9–95.4)	59.1 (38.5–79.6)	77 (68.2–85.9)
VR	87.9 (76.7–99)	97.4 (93.8–101)	93.5 (84.9–102.2)	94.9 (90–99.8)
VR + axial scan	93.9 (85.8–102.1)	98.7 (96.1–101.2)	93.5 (84.9–102.2)	97.4 (93.8–101)

Note:—CI indicates confidence interval; PPV, positive predictive value; NPV, negative predictive value; MIP, maximum intensity projection; MPR, multiplanar reconstruction; SSD, shaded surface display; VR, volume rendering.

atives, we had 2 mixed plaques and 2 fatty plaques, and 3 of these 4 plaques showed an eggshell calcification. This fact may explain the lack of sensitivity in detecting these ulcers. Several studies in the literature demonstrate how MIP is inefficient in assessing stenosis grade associated with calcified plaques. We can add that it is of no utility when looking for a plaque alteration such as ulceration.

Multiplanar reformations are probably the most simple and commonly applied reformatting methods, and they are based on average values of attenuation of the pixels along the axis of projection.[18,19] The vascular MPR image is not 3D but 2D. In the experimental study by Addis et al[30] that used a phantom to assess grade of stenosis with different reconstruction techniques, MPR proved to be less effective compared with other tools. Other studies underlined the importance of MPR use, in particular, in the curvilinear reconstruction

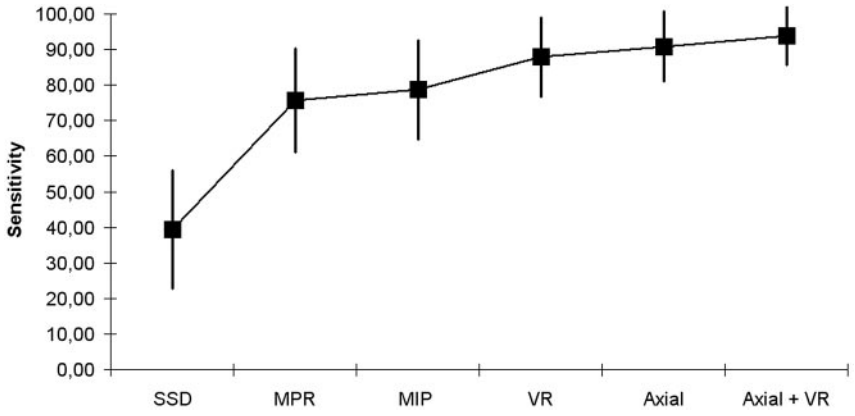

Fig 4. Graph shows the sensitivity of SSD, MPR, MIP, VR, axial, and axial + VR. Mean values (■) and 95% confidence intervals (*error bars*) are indicated

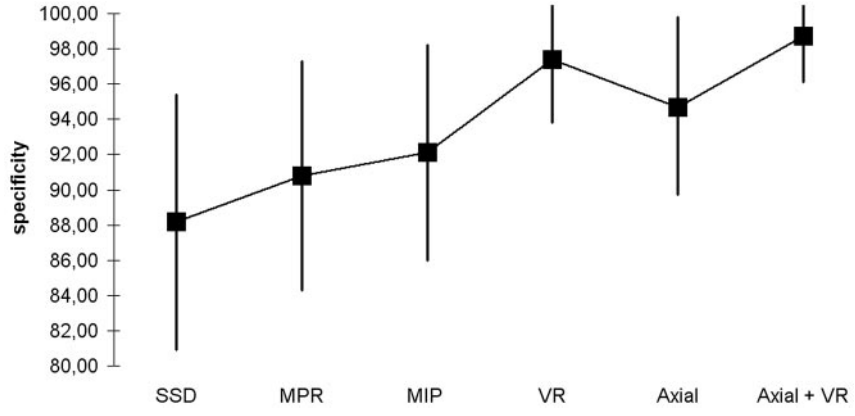

Fig 5. Graph shows the specificity of SSD, MPR, MIP, VR, axial, and axial + VR. Mean values (■) and 95% confidence intervals (*error bars*) are indicated

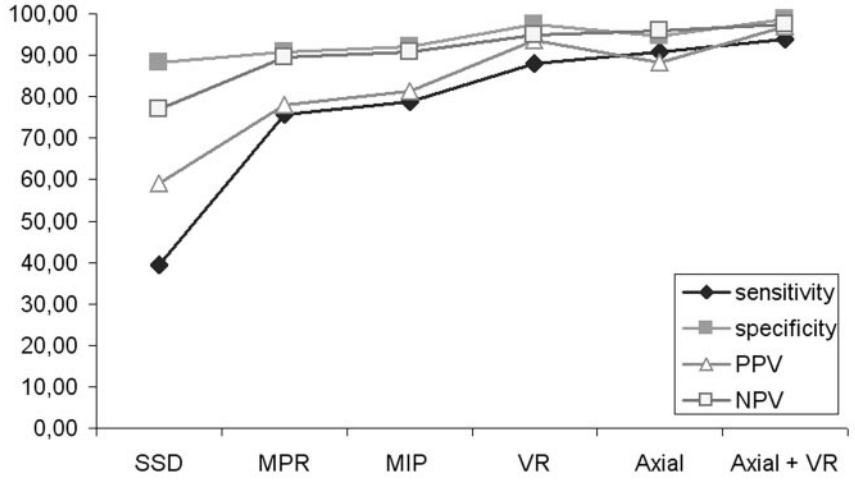

Fig 6. Graph shows sensitivity, specificity, PPV, NPV of SSD, MPR, MIP, VR, axial, and axial + VR.

Table 2: Correlation between stenosis degree and plaque ulceration

Stenosis Degree (NASCET)	Patients with Plaque Ulceration	Patients without Ulceration	% with Plaque Ulceration
50–69 %	1	6	14.29
70–84 %	8	26	23.54
85–99 %	22	46	32.35

Note:—NASCET indicates North American Symptomatic Carotid Endarterectomy Trial.

Table 3: Correlation between plaque type and ulceration

Plaque Type	Patients with Plaque Ulceration	Patients without Ulceration	% with Plaque Ulceration
Fatty	19	16	54.3
Mixed	8	34	19.1
Calcified	4	28	12.5

planes that skip vessel wall calcifications by producing a precise definition of the lumen.[15,31] For the assessment of carotid plaque ulcerations, MPR technique is somewhat inferior to MIP (75.8% versus 78.8% sensitivity). Even MPR, like MIP, does not do well in detecting ulcers in calcified plaques.

SSD is a process in which apparent surfaces are determined within the volume of data and an image, representing the derived surfaces, is displayed. With SSD, specific attenuation thresholds are selected and only portions of the data have been used, giving no information about structures inside or behind the surface. In our study, SSD reconstructions showed inferior

results (Figs 4–6). In particular, sensitivity and PPV proved to be poor. Ulcerations detected with SSD were found in fatty and mixed plaques, whereas the smallest ones were not evidenced.

VR is one of the most advanced and computer-intensive rendering algorithms available, and it incorporates all the relevant data into the resulting image, producing high-quality 3D angiographic images. Other studies analyzed the efficacy of this technique for the evaluation of the grade of carotid stenosis but, to our knowledge, no studies have assessed the capacity of VR to detect carotid plaque ulcerations. In our study VR reconstructions showed high reliability in detecting ulceration. We used 3 trapezoids according to necessity: one for the calcifications, another for the lumen, and the last for contrast medium. This approach, in our study, showed excellent results. We observed also that VR allows a precise plaque assessment even if there are complex plaque calcifications (Fig 3*B–D*). We had difficulties when there were one or more calcifications with low HU values. In this case, the HU plaque value is similar to those produced with endoluminal contrast medium. If we used a calcification histogram, that calcification would not be detected, whereas it was visible when we applied contrast medium histogram. So, if we use a parietal histogram and we do not observe a solution of continuity, we are not likely to observe an ulceration; on the other hand, if there is solution of continuity, we are most likely in the presence of an ulceration. Only with VR images does it become almost impossible to distinguish low HU-grade parietal calcifications that lie in the vessel wall, because during the reconstruction process, they produce images similar to those of the ulceration. Assessment is possible by checking precontrast axial scans and determining whether plaque ulcerations are present in that position.

If we analyze the diagnostic efficacy of the various reconstruction techniques, focusing on the plaque type, our observations lead us to believe that the most difficult type of plaque to analyze is definitely the calcified type or plaques in which calcifications are present. Presence of ulcers in the calcified plaque *type* is quite unusual (Table 3), but, on the other hand, calcification is frequently present in the fatty and mixed plaque types, in which the incidence of ulceration in the plaque is higher (Table 3). By using MIP, MPR, and SSD postprocessing methods, calcifications can hide some small ulcerations as a result of the very high linear attenuation coefficient (μ); to detect it in a calcified plaque or in a plaque in which the calcification is disposed in a eggshell configuration may be very difficult. Axial scans and VR are the only methods, in our experience, with adequate sensitivity. Using the other postprocessing tools, as reported by other authors,[26,32] calcified plaque could be a limitation in determining plaque morphology and in defining the presence of ulcerations. If the ulcer is located in a plaque with eggshell calcification, MPR may detect it, but a correct planes orientation is fundamental to correctly identify it. Consequently we have to consider some points about plaque's type classification. In fact, we divided into 3 groups the possible types of plaque (fatty, mixed, calcified), but if calcium is present in the plaque (even if a small percentage), and particularly if it is in the form of eggshell calcifications, it may create problems for correct plaque visualization. Therefore, to describe the plaque type relative only to the dominant component may not always be sufficient; we think it is preferable to consider the presence of calcification and its spatial disposition. We have not further discussed the incidence and frequency of ulceration relative to plaque type and to degree of stenosis because we have already described this topic in another work.[33]

Based on previous angiographic work,[34] we divided ulcerated carotid plaques into 3 morphologic types: perpendicular, button of shirt, and hook. We observed that perpendicular ulcers are the smallest (6/10 $<$ 2 mm), whereas the button-of-shirt type (Fig 2) ulcers are the biggest (4/13 $>$ 3 mm).

In the diagnosis of carotid ulcerations studied with CTA, it is mandatory to consider the physiopathology of atheromatous carotid plaque. Atheromatous plaque is an active process subject to remodelling and deformation. These changes may determine irregularity in plaque morphology. According to our experience, this situation may produce on CT imaging some types of images that could be mistaken for ulcers by radiologists, particularly if we have uncertain pictures of small dimensions. The presence of a little "in plus image" may be correlated with a plaque fissuration. Other times it is possible to observe the presence of thrombus formation on the surface of a damaged plaque, which further modifies the morphology. For all these reasons, we have empirically considered the presence of atherosclerotic wall thickening into which the ulcer projects as criterion to consider a suspected image as ulcer of plaque. Another parameter we used to define a plaque as ulcerated was the "in plus" image *dimension*: the larger it was, the greater the possibility that an ulcer was present. We considered any entity larger than 1 mm an ulceration.

In this study, some limitations are present. First of all, we used direct visualization of the surgical specimen as a reference standard: histopathologic examination would have been a more accurate "gold standard." The second potential limitation is that vascular surgeons were not blinded about the presence or absence of ulcerations in the carotid artery. Moreover, some plaques, in particular fatty plaques complicated with subintimal hemorrhage, could be very difficult to extract. Because of this situation, in some patients it was impossible to perform CEA en bloc and to study plaque morphology. These patients/plaques were not included in the 109 patients described because it was not possible to obtain surgical data, and this may introduce a further bias.

Conclusions

The results of this study showed that axial scans and various reconstruction methods had different specificity and sensitivity in the study of plaque ulceration; our data suggest that CTA study of ulcerated carotid plaque should be based on axial scans and VR reconstructions. In fact, VR is the most efficient reconstruction technique and when this is associated with axial scans, it is possible to obtain very high specificity and sensitivity values. In some cases, such as plaques without calcifications, the use of MIP and MPR may be adequate to detect the presence of plaque ulceration.

References

1. Robins M, Baum H. **The National Survey of Stroke. Incidence.** *Stroke* 1981; 12(2 Pt 2 Suppl 1):I45–I57
2. Gibbs RGJ, Todd JC, Irvine C, et al. **Relationship between the regional and**

national incidence of transient ischemic attack and stroke and performance of carotid endarterectomy. *Eur J Vasc Surg* 1998;16:47–52
3. Adelman SM. **The National Survey of Stroke. Economic impact.** *Stroke* 1981; 12(2 Pt 2 Suppl 1):I69–87
4. Park AE, McCarthy WJ, Pearce WH, et al. **Carotid plaque morphology correlates with presenting symptomatology.** *J Vasc Surg* 1998;27:872–78
5. Ballotta E, Da Giau G, Renon L. **Carotid plaque gross morphology and clinical presentation: a prospective study of 457 carotid artery specimens.** *J Surg Res* 2000;89:78–84
6. North American Symptomatic Carotid Endarterectomy Trial Collaborators. **Beneficial effect of carotid endarterectomy in symptomatic patients high with grade stenosis.** *N Engl J Med* 1991;325:445–53
7. Kim DI, Lee SJ, Lee BB, et al. **The relationship between the angiographic findings and the clinical features of carotid artery plaque.** *Surg Today* 2000;30:37–42
8. Randoux B, Marro B, Koskas F, et al. **Carotid artery stenosis: prospective comparison of CT, three-dimensional gadolinium-enhanced MR, and conventional angiography.** *Radiology* 2001;220:179–85
9. Runge VM, Kirsch JE, Lee C. **Contrast-enhanced MR angiography.** *J Magn Reson Imaging* 1993;3:233–39
10. Streifler JY, Eliaziw M, Fox AJ, et al. **Angiographic detection of carotid plaque ulceration: comparison with surgical observations in to multicenter study.** *Stroke* 1994;25:1130–32
11. Walker LJ, Ismail Á, McMeekin W, et al. **Computed tomography angiography for the evaluation of carotid atherosclerotic plaque: correlation with histopathology of endarterectomy specimens.** *Stroke* 2002;33:977–81
12. Hessel SJ, Adams DF, Abrams HL. **Complications of angiography.** *Radiology* 1981;138:273–81
13. Herzig R, Burval S, Krupka B, et al. **Comparison of ultrasonography, CT angiography, and digital subtraction angiography in severe carotid stenosis.** *Eur J Neurol* 2004;11:774–81
14. Marcus CD, Ladam-Marcus VJ, Bigot JL, et al. **Carotid artery stenosis: evaluation at CT angiography with the volume rendering technique.** *Radiology* 1999;211:775–80
15. Corti R, Alerci M, Wyttenbach R, et al. **Usefulness of multiplanar reconstructions in evaluation of carotid CT angiography**. *Radiology* 2003;226:290–91
16. Leclerc X, Godefroy O, Lucas C, et al. **Internal carotid artery stenosis: CT angiography with volume rendering.** *Radiology* 1999;210:673–82
17. Cinat Me, Pham H, Vo D, et al. **Improved imaging of carotid artery bifurcation using helical computed tomographic angiography.** *Ann Vasc Surg* 1999;13:178–83
18. Cody DD. **AAPM/RSNA physics tutorial for residents: topics in CT. Image processing in CT.** *Radiographics* 2002;22:1255–68
19. Napel S, Rubin GD, Jeffrey RB Jr. **STS-MIP: a new reconstruction technique for CT of the chest.** *J Comput Assist Tomogr* 1993;17:832–38
20. Prokop M, Shin HO, Schanz A, et al. **Use of maximum intensity projections in CT angiography: a basic review.** *Radiographics* 1997;17:433–51
21. Johnson PT, Heath DG, Kuszyk BS, et al. **CT angiography with volume rendering: advantages and applications in splanchnic vascular imaging.** *Radiology* 1996;200:564–68
22. Ota H, Takase K, Rikimaru H, et al. **Quantitative vascular measurements in arterial occlusive disease.** *Radiographics* 2005;25:1141–58
23. Schroeder S, Kopp AF, Baumbach A, et al. **Noninvasive detection and evaluation of the atherosclerotic plaque with multislice computed tomography.** *J Am Coll Cardiol* 2001;37:1430–35
24. Oliver TB, Lammie GA, Wright AR, et al. **Atherosclerotic plaque at the carotid bifurcation: CT angiographic appearance with histopathologic correlation.** *AJNR Am J Neuroradiol* 1999;20:897–901
25. Lovett JK, Gallagher PJ, Hands LJ, et al. **Histological correlates of carotid plaque surface morphology on lumen contrast imaging.** *Circulation* 2004;110:2190–97
26. Lovett JK, Gallagher PJ, Rothwell PM. **Reproducibility of histological assessment of carotid plaque: implications for studies of carotid imaging.** *Cerebrovasc Dis* 2004;18:117–23
27. Schwartz RB, Jones KM, Chernoff DM, et al. **Common carotid artery bifurcation: evaluation with spiral CT. Work in progress.** *Radiology* 1992;185:513–51
28. Debernardi S, Martincich L, Lazzaro D, et al. **CT angiography in the assessment of carotid atherosclerotic disease: results of more than two years' experience.** *Radiol Med* 2004;108:116–27
29. Link J, Brossmann J, Grabener M, et al. **Spiral CT angiography and selective digital subtraction angiography of internal carotid artery stenosis.** *AJNR Am J Neuroradiology* 1996;17:89–94
30. Addis KA, Hopper KD, Iyriboz TA, et al. **CT angiography: In vitro comparison of five reconstruction methods.** *AJR Am J Roentgenol* 2001;177:1171–76
31. Corti R, Ferrari C, Roberti M, et al. **Spiral computed tomography: a novel diagnostic approach for investigation of the extracranial cerebral arteries and its complementary role in duplex ultrasonography.** *Circulation* 1998;98:984–89
32. Cumming MJ, Morrow IA. **Carotid artery stenosis: to prospective comparison of CT angiography and conventional angiography.** *AJR Am J Roentgenol* 1994;163:517–23
33. Saba L, Caddeo G, Sanfilippo R, et al. **CT and US in the study of ulcerated carotid plaque compared with surgical results. Advantages of multi-detector-row CT angiography.** *AJNR Am J Neuroradiol* 2007; In press
34. Lovett JK, Gallagher PJ, Hands LJ, et al. **Histological correlates of carotid plaque surface morphology on lumen contrast imaging.** *Circulation* 2004;110: 2190–97